Zachary Gagnon
Hsueh-Chia Chang

Center for Microfluidics and Medical Diagnostics, Department of Chemical and Biomolecular Engineering, University of Notre Dame, Notre Dame, IN, USA

Aligning fast alternating current electroosmotic flow fields and characteristic frequencies with dielectrophoretic traps to achieve rapid bacteria detection

Tailor-designed alternating current electroosmotic (AC-EO) stagnation flows are used to convect bioparticles globally from a bulk solution to localized dielectrophoretic (DEP) traps that are aligned at the flow stagnation points. The multiscale trap, with a typical trapping time of seconds for a dilute 70 μL volume of 10^3 particles *per* cc sample, is several orders of magnitude faster than conventional DEP traps and earlier AC-EO traps with parallel, castellated, or finger electrodes. A novel serpentine wire capable of sustaining a high voltage, up to 2500 V_{RMS}, without causing excessive heat dissipation or Faradaic reaction in strong electrolytes is fabricated to produce the strong AC-EO flow with two separated stagnation lines, one aligned with the field minimum and one with the field maximum. The continuous wire design allows a large applied voltage without inducing Faradaic electrode reactions. Particles are trapped within seconds at one of the traps depending on whether they suffer negative or positive DEP. The particles can also be rapidly released from their respective traps by varying the frequency of the applied AC field below particle-distinct cross-over frequencies. Zwitterion addition to the buffer allows further geometric and frequency alignments of the AC-EO and DEP motions. The same device hence allows fast trapping, detection, sorting, and characterization on a sample with realistic conductivity, volume, and bacteria count.

Keywords: Bacteria; Dielectrophoresis; Electrokinetics; Microfluidics
DOI 10.1002/elps.200500129

1 Introduction

1.1 General aspects

In the last decade, the advent of microfluidic research has spawned a new array of lab-on-a-chip technologies operating at length scales typically on the order of tens of microns. Indeed, much time has been spent on developing the essentials, such as micropumps, micromixers, microvalves, and microchannels, for an effective portable microfluidic kit. However, there has been relatively little success in developing portable technologies that can rapidly detect, distinguish, and analyze dilute solutions of bioparticles such as bacteria or viruses.

Correspondence: Professor Hsueh-Chia Chang, 182 Fitzpatrick Hall, Department of Chemical Engineering, University of Notre Dame, Notre Dame, IN 46556, USA
E-mail: hchang@nd.edu
Fax: +1-574-631-8366

Abbreviations: **AC-EO**, alternating current electroosmotic; **AHA**, 6-aminohexanoic acid; **CFU**, colony-forming units; **CM**, Clausius–Mossotti; **COF**, cross-over frequency; **DI**, deionized; **DEP**, dielectrophoresis; **n-DEP**, negative dielectrophoresis; **p-DEP**, positive dielectrophoresis

Current bioparticle analysis techniques typically rely on labor-intensive culturing or PCR amplification to first increase the concentration of a dilute sample. Culturing is then routinely followed by a relatively fast and accurate assay involving fluorescent antibodies, magnetic beads, or fluorescent nanoprobes. While such tests are usually quick, taking several minutes, they are still limited by the time and effort required, usually 1–7 days, to culture or amplify a dilute sample. Typical bacteria counts in medical and environmental samples are on the order of only 100 colony-forming units (CFU) *per* cc, while the present benchmark required for lab analysis is no less than 10 000 CFU/cc [1]. Therefore, significant improvements in detection signal amplification are required before it becomes possible to develop a truly portable and rapid microfluidic bioparticle detection kit.

One possible means of amplifying the bacteria or virus signal is to concentrate the bioparticles at a specific location in order to magnify the fluorescent intensity or electrochemical signal of the sample. Over the past 10 years there has been significant interest in utilizing dielectrophoresis (DEP) forces generated by microelectrodes in order to capture and concentrate charged bio-

particles in suspension. DEP has been successfully used to capture a range of bioparticles such as viruses, DNA, and proteins [2–9]; however, there are still many disadvantages in the current DEP trapping techniques. Many of these authors report relatively fast bioparticle trapping times, on the order of a few seconds, however their technique typically involves placing cells in the vicinity of the trap, where upon activation, they are immediately attracted to a local DEP trap and concentrated. If the sample is highly dilute ($<$1000 CFU/cc) however, or if one has a large volume of fluid to process, this current technique will usually lead to infeasible processing times.

Limitations in processing times stem from the fact that the DEP velocity of a particle is small, and can be shown to scale quadratically with particle radius and linearly with the applied voltage. The quadratic dependence on the particle radius and practical limitations on the applied voltage render the particle velocity produced by a DEP force miniscule, typically on the order of 10 μm/s for bacteria and 1 μm/s for viruses, and usually leads to a concentration time on the order of hours. Also, the field gradient necessary to drive DEP motion can only be achieved with relatively narrow interdigitated electrodes whose field penetration depth is also limited by the electrode width. As a result, DEP channels are usually less than 50 μm in transverse dimension. Therefore, slow capture and small transverse dimensions are responsible for extremely low throughputs in current continuous flow kits.

Due to the above limitations, there is considerable interest in replacing or augmenting DEP traps with alternating current electroosmotic (AC-EO) flows to increase the volume of fluid that the trap can act on. Such flows are due to field-induced polarization on the AC electrode surface and are not dependent on the particle dimension. They convect the particles by viscous drag and hence can endow the particle with the flow velocity. As such, they are, at least in theory, of longer range and can impart a higher particle velocity than DEP designs [8, 10]. Green *et al.* [11] have investigated in detail microfluidic flows on the surface of a coplanar electrode pair, documented AC-EO flow rates as a function of electrolyte conductivity, signal frequency and potential, and position on the electrode surface.

However, convection by AC-EO alone is not sufficient to trap bioparticles. The particle trajectory would be identical to the AC-EO streamline and due to the volume-conservation property of incompressible flow, none of the stagnation points of the flow field would be attracting – they are either hyperbolic saddle points or elliptic centers. The electrode surface itself is also a slip plane due to the AC-EO slip velocity, although saddle-point stagnation lines or points could appear. The optimal design would be to impose yet another field on the particles at the electrode stagnation points or lines, where the viscous drag is weakest, such that the stagnation points or lines become attracting and can perform as a multiscale bioparticle trap. Such a local field near the stagnation point/line can be a DEP field, as in the case of [2–9], or other short-range local particle forces like gravity or magnetic force.

The purpose of this work is to introduce a new wire trapping design and buffer solution selection to enhance bioparticle concentration, detection, and manipulation of dilute solutions of bioparticles. Bioparticles are not locally trapped on disjoint microelectrodes, but rather they are convected from a bulk solution by a pair of asymmetric vortices across a coplanar serpentine wire, with a large voltage drop and surface polarization, to local DEP traps on the substrate where the local particle force fields can be tangentially attracting. In this manner, both diverging and converging stagnation flows are rendered effective, and rapid traps and the device acts on a much larger volume of fluid than existing DEP technology.

The challenge in rapid global trapping is to align the substrate and electrode stagnation lines of an AC-EO flow with that of a local electric field minima or maxima such that bioparticles are now rapidly convected from the bulk solution to the substrate surface where they are trapped in one of the traps by a local negative or positive DEP (n- or p-DEP) force. Rapid particle sorting of live and dead cells by DEP direction is hence achieved. Zwitterion addition to the buffer also enhances the AC-EO stagnation flow and allows one to achieve optimal trapping conditions by changing the dielectric and surface-conducting properties of the strong electrolyte.

When a dilute aqueous suspension of polymer microspheres, or biological cells such as bacteria, is exposed to an AC electric field, electrical forces can act both on the particles and the surrounding fluid. For AC fields, the governing electrical force acting on a particle is DEP. The electrical force acting on the fluid leads to what is commonly referred to as AC electroosmosis.

1.2 DEP

The classical DEP theory [12, 13] produces a DEP velocity of the form

$$u_{\mathrm{DEP}} = \frac{1}{3\mu}\,\varepsilon_m r^2 Re[K(\omega)]\nabla|E|^2 \qquad (1)$$

where for a homogeneous spherical particle, $K(\omega) = (\varepsilon_p^* - \varepsilon_m^*)/(\varepsilon_p^* + 2\varepsilon_m^*)$ is the Clausius–Mossotti (CM) factor, and $\varepsilon^* = \varepsilon - \sigma/\omega$ is the complex permittivity which is dependent on σ, the conductivity, and ω, the applied field frequency. The imaginary part is out of phase with the applied field and, to first order, can be experimentally

determined by measuring the torque on a particle in electrorotation experiments [5]. However, the real part of the CM factor is in phase with the applied field and describes the particles polarizability and field-induced dipole moment [6].

A more complex polarization model [14] that includes a conducting Stern layer around the particle surface can be shown to modify the effective particle conductivity and permittivity yielding an effective complex particle permittivity in the form

$$\varepsilon_p* = (\varepsilon_p + \varepsilon_{dl}2\lambda/R) - j(4\pi/\omega)(\sigma_p + \sigma_{dl}2\lambda/R) \quad (2)$$

where λ is the thickness of the stern layer. From the above expressions the charge relaxation time for the particle can be shown to be [14]

$$\tau = \frac{2\varepsilon_p + \varepsilon_m + \varepsilon_{dl}2\lambda/R}{(2\sigma_m + \sigma_p + \sigma_{dl}2\lambda/R)} \quad (3)$$

It is well known that u_{DEP} changes sign at the cross-over frequency (COF), $1/2\pi\tau$ [4, 13] where the CM factor $K(\omega)$ vanishes. For most bacteria, $Re[K(\omega)]$ is negative for $\omega >$ COF and the particles move towards the low field region (n-DEP). p-DEP occurs for $\omega <$ COF. It is interesting to note that both the particle size, R, and the double layer thickness, $\lambda = (\varepsilon RT/^2z2Fc_o)^{1/2}$, appear in the COF only if a conducting Stern layer is included. In fact, when the double layer is thin at high concentrations and low permittivities, it can be shown that COF $\sim 2\pi\sigma_m/\varepsilon_m = 2\pi D/\lambda^2$ for $(\sigma_m/\sigma_{dl}) \gg (\lambda/R)$. Conversely, in the limit of $(\sigma_m/\sigma_{dl}) \ll (\lambda/R)$, COF $\sim 2\pi\sigma_m/\varepsilon_m = 2\pi D/\lambda R$ is particle size-dependent.

1.3 AC-EO

AC-EO flow is typically produced with two planar parallel microelectrodes in contact with an electrolyte solution. When an AC voltage is placed between these two electrodes an electric field is produced, which interacts with the electrolyte ions, and in the absence of charge injection, or Faradaic reactions, the electrode surface is polarized by counterions in the electrolyte to form a field-induced electrical double layer. Because the double layer is essentially charged like a capacitor, this particular charging mechanism is typically referred to as capacitive charging.

Based on the work by Gonzalez *et al.* [15], the time-averaged slip velocity on the electrode is

$$u_{AC-EO} = -\frac{\varepsilon_m}{4\mu}\frac{\partial}{\partial x}|\phi - V_0|^2 \quad (4)$$

where ϕ is the value of the potential at any given location above the electrode surface and V_0 is the potential applied to the electrode. The equation represents the effective slip velocity on the electrode surface. If values of the electric field are known, the bulk fluid velocity can now be solved using the Navier–Stokes equation with Eq. (4) as a boundary condition. The electric field on the electrode surface is frequency-dependent and can be shown to be

$$\sigma\frac{\partial\phi}{\partial y} = i\omega C_{DL}(\phi - V_0) \quad (5)$$

which is nothing more than a charge balance in the normal direction across the double layer, where $C_{DL} \sim \varepsilon/\lambda$ is the capacitance *per* unit area of the total double layer. The time-averaged electric field can now be solved using the Laplace equation with Eq. (4) as a boundary condition, and using Eq. (5) together with the Navier–Stokes equation the complete hydrodynamic-electrical problem can be solved.

Using typical values of electrolyte conductivity and permittivity (σ = 100 mS/cm, ε_m = 80), the normalized fluid slip velocity is shown as a function of signal frequency in Fig. 1. It is evident that theory predicts an optimum frequency where a maximum in slip velocity exists. This can be argued from the physical reasoning. Because ion migration to the surface of each electrode requires a finite amount of time, the electrode charging dynamics will have some dependence on the applied AC signal frequency. This dependence can be estimated by simple scaling arguments. The circuit equivalent to the electrode system can be approximated as a double layer capacitor, with charge separation over a length λ, in series with a bulk fluid resistor. The resulting RC charging time for this equivalent resistor-capacitor in series is simply $\lambda L/D$, where L is the electrode separation. Hence, there is an optimum frequency at which one observes a maximum AC-EO flow.

At frequencies below $D/\lambda L$, the half-cycle is long enough such that counterions have enough time to completely saturate the double layer, effectively shielding the electric field from the bulk solution. Additionally, at frequencies above $D/\lambda L$, the counterions do not have enough time to migrate to the electrode surface and form a double layer. Since the time-averaged electrokinetic flow requires both double layer polarization and external field, it must vanish at these two extremes and a maximum AC electrokinetic velocity should occur at a frequency of $D/L\lambda$.

1.4 DEP/AC-EO trapping

It is clear from Eq. (4) that a stagnation line exists in the flow field when the tangential electric field vanishes. Ben and Chang [16] have shown that, for capacitive charging on two symmetric planar electrodes, this stagnation line occurs at the center of the electrode at frequencies lower

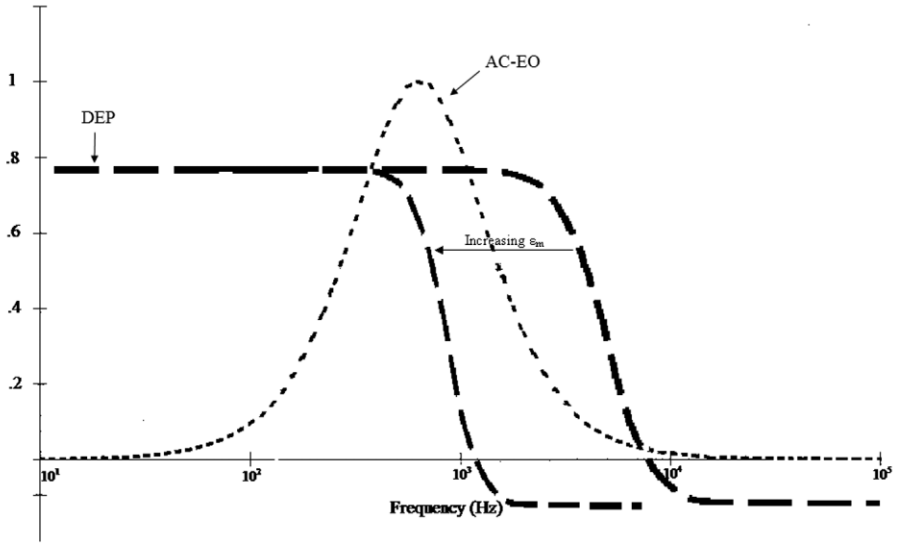

Figure 1. Real part of the CM factor, representing DEP direction, superimposed on AC-EO slip velocity. Electrolyte permittivity increase shifts Re[$K(\omega)$] to the left into a region of stronger AC-EO flow.

than $D/L\lambda$. For frequencies near or higher than $D/L\lambda$, the stagnation line shifts toward $1/\sqrt{2}$ of the width as measured from the inner electrode edge.

It is evident that the AC-EO slip velocity is larger than the DEP velocity by a factor of $(L/a)^2$. Since the electric field on any electrode is higher than that of the surrounding medium, and since most particles are of low permittivity compared to a surrounding aqueous solution, they exhibit a p-DEP force at frequencies near $D/L\lambda$, when the capacitive charging electrokinetic flow is most robust. Therefore, because strong electroosmotic convection forces exist under conditions in which particles exhibit p-DEP, and the flow stagnation lines are aligned with that of a high field region, one would expect particles to be convected from the bulk electrolyte and trapped at the converging stagnation line on the high field electrode surface. Additionally, the field between the two electrodes is generally weak and hence represents an n-DEP trap. Hence, if operating at frequencies above the COF of the particle, and assuming strong electroosmotic flow still exists, one would also expect the particles to be trapped in the gap at high frequencies when the particles suffer from n-DEP.

1.5 Concentration/separation requirements

It is important to note that DEP and AC-EO typically suffer from widely differing charge relaxation times, and it is for this reason that rapid particle separation or rapid n-DEP trapping, on the order of seconds, has not been feasible. The DEP COF of a particle is directly related to the charge relaxation time of the particle, which is usually much shorter than the charge relaxation time for AC-EO flow. In fact, the typical COFs for common types of particles and bacteria exist where AC-EO flow has tended toward zero [4, 11]. Rapid particle concentration requires both strong AC convection and particles operating under p-DEP or n-DEP. Because most particles exhibit n-DEP at high frequencies where electroosmotic flow is weak, convection-enhanced particle trapping is typically not possible when particles are operating under n-DEP. This detail places limits on current DEP traps. The majority of biological samples used today contain multiple species of bacteria, cells, and waste products. Rapid particle concentration is not practical if the collected sample requires hours of careful preparation, or if the collection device simply collects everything in the sample on an electrode. Eventually, some sort of particle separation would be required either before, during, or after particle trapping had occurred. The current problem is that the rapid separation of a multiparticle sample requires strong electroosmotic convection at frequencies where some particles are operating under p-DEP and other exhibit n-DEP, and as explained before, the difference in charge relaxation times between DEP and electroosmotic phenomena in typical electrolyte solutions prevent this.

The most obvious solution to the separation problem is to shift the CM factor to the left, towards the optimum AC-EO frequency, or the converse, to shift the electroosmotic velocity curve to the right. It has been shown that by increasing the conductivity of the electrolyte solution, one can shift the optimum electroosmotic frequency to the right [11], however this usually leads to a decrease in AC-EO slip velocity.

Another possibility is to modify the CM factor such that the COF of a bioparticle is reduced and exists at a frequency where AC-EO is strong. From Eq. (1), it is clear

that if one increases the electrolyte permittivity, the Maxwell–Wagner relaxation frequency will decrease. This can be argued physically in that if the electrolyte permittivity is increased, the number of ions that accumulate on the particle surface for the first half-cycle increases. During the second half-cycle, these ions must migrate around the particle in order for the dipole to change direction. However, because the ion density has increased, it now will take a longer amount of time for the ions to equilibrate and the dipole moment to reverse direction, thus leading to an increased relaxation time or a decreased COF. Therefore, one possible way to reduce bioparticle COF is to increase the permittivity of the electrolyte solution.

The relaxation time for AC-EO is also dependent upon the permittivity of the medium in that $\lambda L/D$ can be shown to scale as ε/σ, where σ is the conductivity of the medium. It is clear that an increase in permittivity will shift the optimum electroosmotic frequency further away from the DEP COF. However, while the magnitude of the DEP force acting on a particle is dependent on electrolyte conductivity, the polarizability of the medium depends largely on a solutions permittivity. Therefore, in order to achieve an optimum balance of both DEP and convection forces, one simply needs to increase the electrolyte permittivity, which will decrease a suspending particles COF, and increase the electrolyte conductivity to counteract the increase in electroosmotic relaxation time. As shown in Fig. 1, a desired separation can most rapidly take place when the COF exists at or near the optimum electroosmotic frequency.

Increasing electrolyte permittivity is quite straightforward. It has been shown that the electrical permittivity of a suspending fluid can be increased by adding ionic molecules, or zwitterions, of high polarizability to an aqueous solution. For example, Arnold and Zimmerman [17] have shown that the addition of 2 mol of a glycine peptide to water increases it relative permittivity by ~252, reducing the Maxwell–Wagner relaxation frequency by ~25%.

1.6 Device design

It is clear from the above discussion that, while AC-EO traps should function better than DEP traps, the limitation to low voltages and low-conductivity fluids renders them quite ineffective. The low voltage requirement stems from the fact that, for disjoint electrodes, Faradaic reactions will eventually occur at sufficiently high voltages and low frequencies. This is because the field for disjoint electrodes must cross the electrode/electrolyte interface and, with sufficient voltage drop and sufficient reaction time, will induce an electrode reaction. As thin as the double layer is for strong electrolytes, a sufficiently large electric field should still produce strong AC-EO flow. Hence, limitation to weak electrolytes can be alleviated if Faradaic reaction can be avoided such that a high rms voltage can be applied.

In this work, we remove both limitations by discarding the disjoint electrode design. Instead, a continuous serpentine wire is used such that most of the AC current passes through the wire and not the electrolyte. Large voltage drop exists along the wire to produce enormous capacitive charging on the wire surface but without a significant field across the electrode-electrolyte surface. With this design, capacitive charging up to 2500 V_{RMS} can be achieved to produce AC-EO that are orders of magnitude higher than earlier disjoint electrode designs. Bioparticle concentration, separation, and manipulation can now be achieved in large (cc) volume of strong electrolytes.

As shown from a top view in Fig. 2, the microdevice consists of a thin 50/200 nm Ti/Pt wire on an insulated silicon substrate in contact with an aqueous suspension of bioparticles.

Due to the large difference in electrical conductivity between the wire and electrolyte, the applied current will be largely confined to the wire, thereby eliminating any noticeable electrochemical reactions and pH gradients even at high voltages (~ 2500 V_{RMS} AC). There is still a large voltage drop between different segments of the serpentine wire. However, the Faradaic reaction this intersegment voltage would drive is a high-resistance Faradaic resistor in series with the high-capacitance interfacial Stern layer and double layer capacitors. This Faradaic RC circuit is in parallel with the low-resistance wire. Hence, at the high-frequency employed, much higher than the inverse RC time of the Faradaic resistor, almost all the AC current runs through the wire with little AC Faradaic charge transfer. More importantly, because the serpentine wire can sustain such high voltages, the AC-EO flow is still quite robust for high-conductivity electrolytes.

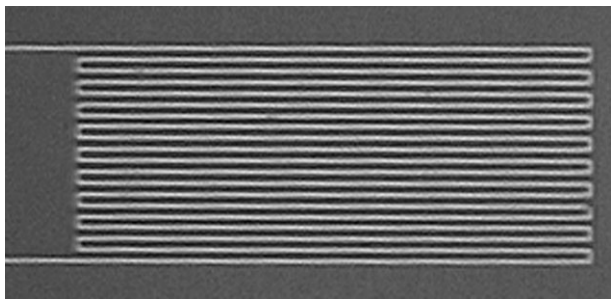

Figure 2. Fabricated DEP/AC-EO trap.

Although the device still has a large heating power from the current in the wire, Joule heating effects are avoided by fabricating the device atop a heat conducting silicon substrate. It will be shown that heat effects on fluid motion, both through Raleigh–Bernard instability and electrothermal effects, are negligible for this design and that this new configuration allows one to achieve much higher fluid velocities and field strengths than existing electrode geometries.

Following earlier work by Gonzalez *et al.* [15], one can solve the Laplace equation for the electric field using Eq. (5) as a boundary condition. The electroosmotic velocity profile is then solved numerically for a cross-section (cut across wires) of the serpentine wire using Eq. (4) on each wire surface. The magnitude of the electric field and the resulting velocity field are shown in Figs. 3A and B, respectively. Numerical simulations were performed using the FEMLAB finite element software package (COMSOL, Burlington, MA, USA).

From a side view of the device shown in Fig. 3A it is clear that the wires on the outer region of the serpentine have the largest field. Additionally, the velocity profile is anti symmetric with a stagnation point near the two outer wires. The important thing to note, superimposing these two figures, is that a converging stagnation line exists directly above a local field minimum on the right-hand side of the device, as shown in Fig. 4.

The left hand side of the device has a small flow stagnation line, however it is not aligned with a local field minimum. Therefore, if operating under the correct electrolyte and frequency conditions, one would expect bioparticles in the bulk solution to be convected directly to a local n-DEP trap on the right-hand side, collecting much faster than the left hand side where the particles are brought only in the vicinity of a field minimum (~40 μm), but not directly upon it. If operating under p-DEP, the particles should be attracted to the wires with the highest field, as they will follow the streamlines and continue to sample the entire device surface. Particle separation can be achieved by noting that the particles suffering n-DEP will be rapidly attracted to the field minimum regions between the wires, while the p-DEP particles will be attracted to the high field wires.

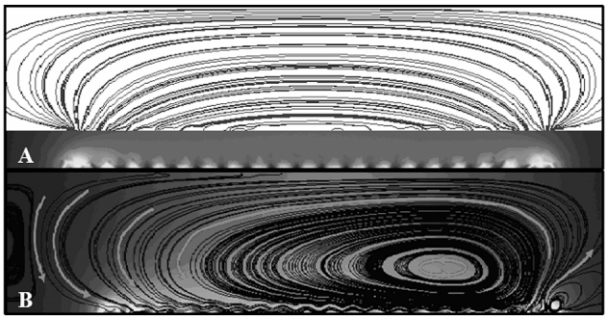

Figure 3. (A) Side view of the theoretical electric field lines of the device at 5 V_{RMS} and 40 kHz showing the highest values in field is predicted on the outer wires. (B) Theoretical fluid streamlines illustrating two converging stagnation lines, one on right edge of the device and the other on the outer left.

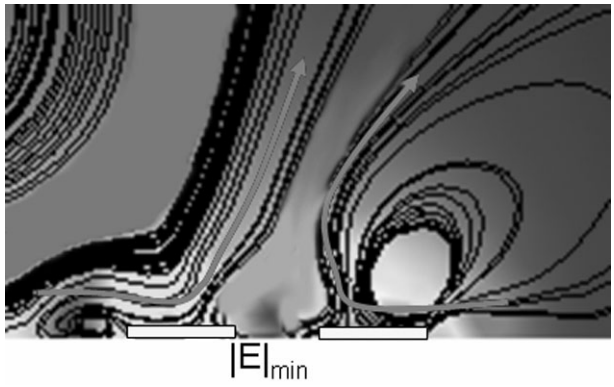

Figure 4. Fluid streamlines with arrows indicating direction superimposed atop electric field contours for the last two wires on the right side of the device illustrating a stagnation line aligned directly atop a field minimum.

2 Materials and methods

Thin-film serpentine platinum wires were fabricated using conventional semiconductor and soft lithography techniques. Briefly, serpentine wire geometries were photopatterned onto a dielectric (SiO_2)-coated silicon wafer. Fifty nanometer titanium/200 nm platinum was then deposited using electron beam evaporation, and the photoresist was then lifted off in an organic solvent to yield thin film wire patterns. The resulting structure consisted of a serpentine structure with wires 35 μm wide and 2500 μm long, arranged in a serpentine structure with a periodicity of 5040 μm, and consisted of ten periods, or 20 parallel wires interconnected at every other end, as shown in Fig. 2.

Experiments were conducted in polymer microchannels which were produced using conventional soft-lithographic techniques. Briefly, microchannel master molds were fabricated using thick SU-8 photoresist (SU8–2075, Microchem, Newton, ME, USA). Uncured polydimethylsiloxane (PDMS) (Sylgard 184, Dow Corning, Midland, MI, USA) was then poured and cured atop the molds, peeled off, and carefully aligned atop the serpentine wire structure. This construction formed a channel that was 500 μm deep, 4000 μm wide, and 3.5 cm long aligned lengthwise

above the wire structure. Fluid entrance and exit ports were made in the polymer channel using a 22 gauge syringe needle. Finally, a 300 μm glass capillary was inserted at the entrance port and attached to a syringe, yielding a sample volume of 70 μL. The port and syringe connections were sealed using a quick dry epoxy resin and the syringe placed in a digitally controlled syringe pump. A new polymer channel was used for each experiment. Particle suspensions were then injected into the microchannel *via* a syringe pump. An AC potential was dropped across the wire structure by a signal generator (Agilent 33220A) connected to an RF amplifier (Powertron Model 250A, Industrial Test Equipment), and the final assembly, as shown in Fig. 5, was then viewed under Fluorescent Microscope for visualization. With reference to the high voltage operation, as mentioned earlier in this work, the power system was further combined with an output transformer (Industrial Test Equipment, P/N 113459–2) capable of outputting up to 2500 VRMS.

Dried bakers yeast cells (Fleishmann Active Dry Yeast) were reconstituted in CO_2-equilibrated deionized (DI) water (12 MΩ × cm, pH 6.5), 1 μm fluorescent polystyrene microparticles and 5 m latex microparticles were obtained from Polysciences (Warrington, PA, USA) and diluted to approximately 10^3 particles *per* mL in DI water. Electrolyte permittivity and conductivity was adjusted by adding varying amounts of the zwitterion 6-aminohexanoic acid (AHA) (Sigma-Aldrich, St. Louis, MO, USA) to a prepared polymer suspension. *Escherichia coli* bacteria (F-amp) diluted in DI water to a concentration of ~ 500 CFU/cc was obtained from Scientific Methods.

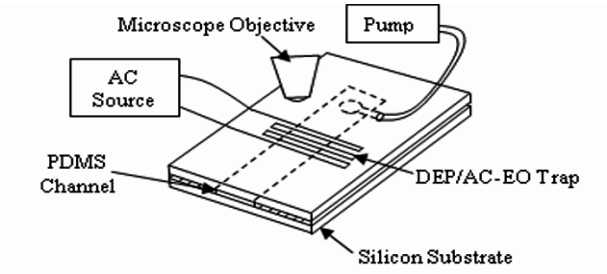

Figure 5. Experimental setup.

3 Results and discussion

Experiments were conducted in order to verify the enhancing effects that AC-EO has on the trapping of bioparticles. The p-DEP behavior, in the absence of convection forces, of 1 μm polystyrene fluorescent microparticles suspended in pure DI water was first investigated. One micrometer particles were used because by conventional DEP theory, small 1 μm particles exhibit p-DEP behavior at low (< 100 kHz) frequencies. A suspension of particles was injected into the microchannel and an AC potential (5 V_{RMS}) was dropped across the wire at a frequency of 40 kHz. Prior to this experiment, the AC-EO fluid velocity was measured as a function of voltage and applied frequency approximately 15 μm above the wire surface for pure DI water using previously described techniques [11]. As shown in Fig. 6, when 5 V_{RMS} is dropped across the wire at 40 kHz, the fluid velocity is weak at approximately 7 μm/s. It should also be noted that the measured fluid velocity scales quadratically with the applied voltage, while electrothermal flow scales as the applied voltage to the fourth power [18]. Additionally, the

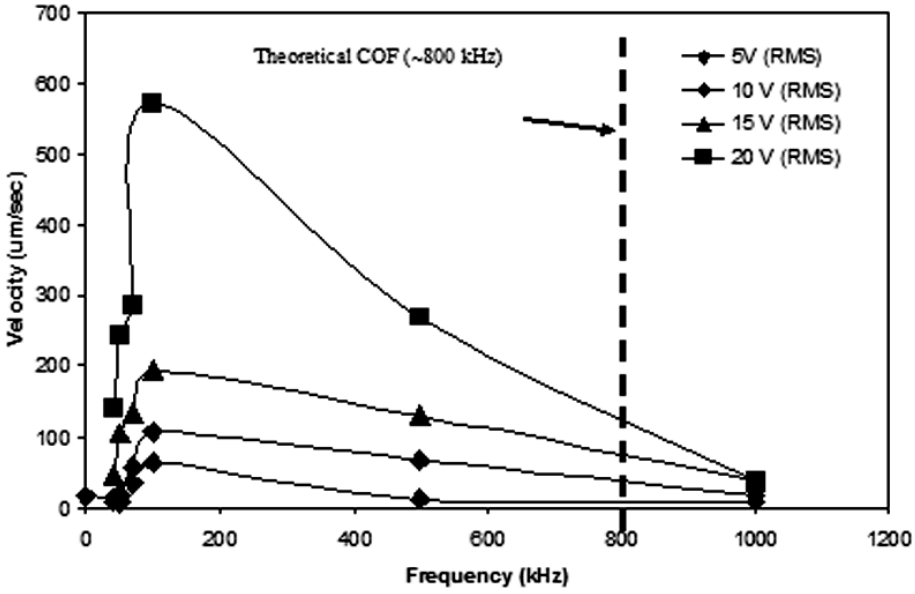

Figure 6. Measured fluid velocity for DI water as a function of AC frequency for four different applied voltages: 5, 10, 15, and 20 V. Predicted COF for DEP is also indicated. It is clear that the n-DEP trap at $\omega >$ COF would not be aided by the weak AC-EO flow at high frequencies.

channel height is ~ 300 m, giving rise to a Raleigh number of ~ 10, well below the critical value required (~ 1707.26) for any flow resulting from a thermal instability [19]. In fact, in order to reach this critical value, one can show that this would require an infeasible temperature gradient on the order of ~15°C/μm. Finally, thermal Joule heating should be uniform along the wire and the vortices they drive are necessarily symmetric in contrast to the highly asymmetric vortex shown in Fig. 3. Therefore, the flow observed experimentally is most likely lateral AC-EO flow.

Figure 7 shows the optical fluorescent microscopy images of the microparticles patterned by p-DEP. This image took approximately 22 min to form, which is consistent with the trapping time of earlier DEP traps that operate at roughly this voltage. It is obvious that the particles (lighter areas on the device) are experiencing a p-DEP force in that they are attracted to the high field regions of the serpentine wire surface. More importantly, they are highly concentrated on the outer high field wires of the serpentine pattern, thus verifying the electric field calculations as shown earlier in Fig. 3A.

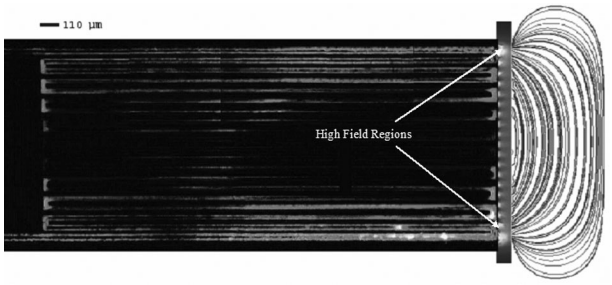

Figure 7. Image of p-DEP trapping of 1 μm fluorescent particles taken 22 min after device activation at 5 V and 40 kHz, calculated field lines/intensity aligned on far right of device.

The n-DEP characteristics of the device in the absence of strong convective forces were also investigated. As mentioned earlier, n-DEP particle collection on the right side of the device should be much faster than conventional n-DEP trapping, without convection, due to the stagnation line that is directly aligned above a local field minimum. A solution of 5 μm latex particles was suspended in DI water and injected into the device. Larger particles were used in this experiment to decrease the particle COF so that n-DEP behavior could be studied. Additionally, a larger voltage was used so that the results of this experiment could be compared to one with zwitterions enhancement. Upon device activation (20 V_{RMS}, 1.2 MHz), particle accumulation in the DEP trap was observed to be slow. There were small amounts of particles collected in n-DEP traps on the device, however these patterns took approximately 30 min to form. From Fig. 6, one can see that at 20 V_{RMS}, the fluid velocity at 1.2 MHz is approximately 40 μm/s, while the calculated DEP velocity can be shown to be approximately 10 μm/s. It is obvious that in order to decrease the time required for collecting particles in the n-DEP traps, one needs to increase the electroosmotic convection fluid velocity or the local field at the stagnation line. We shall do both below by the addition of zwitterions.

A new suspension of 5 μm particles was created using a 1.5 M solution of AHA. The solutions relative permittivity was measured in previous work and shown to be ~ 200 [17], approximately a factor of 2 higher than that of DI water (~ 80). The AC-EO velocity was measured as a function of applied frequency prior to the experiment and is shown in Fig. 8.

As shown in Fig. 8, the optimal frequency is approximately 200 kHz, a factor of 2 higher than that of DI water, while that of the measured electroosmotic velocity is also

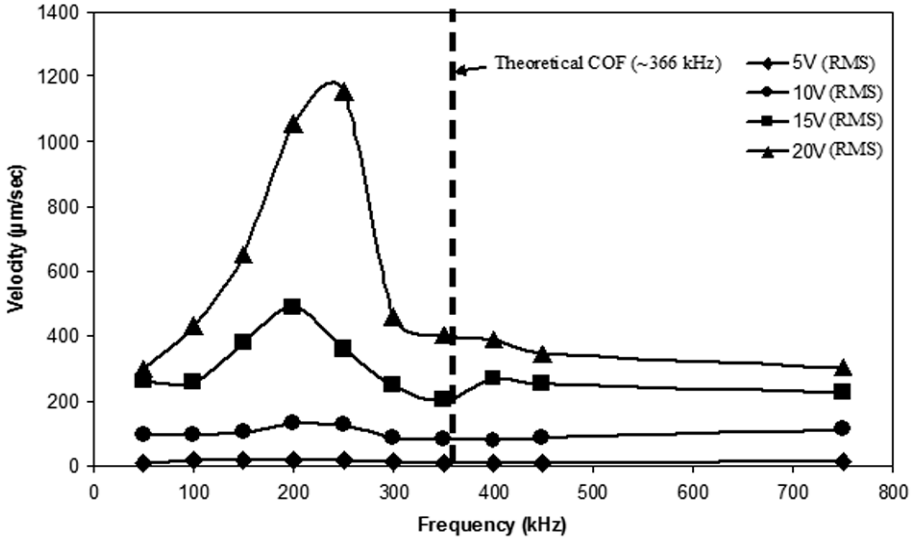

Figure 8. Measured fluid velocity for 1.5 M AHA solution as a function of AC frequency for four different applied voltages: 5, 10, 15, and 20 V. Zwitterions shift COF to much lower frequencies where the AC-EO velocity is a robust 400 μm/s and can help trap particles at the n-DEP trap.

a factor of 2 greater. More importantly, n-DEP can now exist at much lower frequencies where significant AC-EO flow (~ 400 μm/s) can be utilized to accelerate particle trapping. The solution was injected into the device, an AC voltage (20 V_{RMS}) was applied, and the frequency was slowly increased until an n-DEP particle collection was observed. At a frequency of 400 kHz, unlike the slow particle trapping in DI water, rapid n-DEP particle trapping in the stagnation aligned negative field region on the right-hand side of the device was observed. As shown in Fig. 9, trapping time was reduced by two orders of magnitude, taking only 32 s for 5 μm particles to arrange in a highly ordered cubic array of approximately 2500 μm in length. The left-hand side of the device also trapped particles, however the time required to form the complete 2500 μm line took approximately 4 min. The 20 V_{RMS} is beyond most of the earlier AC-EO traps with disjoint electrodes due to the appearance of Faradaic reactions. With the addition of zwitterion, the convection flow is further enhanced as the optimal frequency for AC-EO can now be employed and still allow n-DEP trapping. Moreover, with any significant AC-EO convection, the rate-limiting step is probably the trapping speed at the local field and the addition of zwitterion also amplifies the local n-DEP force.

The observable decrease in particle collection time and increase in fluid velocity is also affected by the permittivity adjustment of the electrolyte. By adding zwitterion to the solution, the electrolyte permittivity was increased and therefore led to a decrease in the particle COF and placed the n-DEP frequency range of the particle in a range where strong electroosmotic flow existed. Additionally, as shown in Eq. (4), the electroosmotic slip velocity is also proportional to the electrolyte permittivity, and the addition of the zwitterion also led to a factor of 2 increase in the observable electroosmotic velocity. Therefore, by simply increasing the permittivity of the electrolyte solution, the frequency at which a particle experienced an n-DEP forced was reduced, driving the particle into an operating range where increased convection forces existed which in turn convected the particle across the channel gap and directly into an n-DEP trap, reducing the required collection time. This concept is further supported by the fact that the aligned stagnation trap on the right side of the device required only seconds to trap particles, while that of the trap on the left side, 100 μm away from a stagnation line, required a much longer time, taking on the order of several minutes.

It is clear from the above experiments that trapping time can be enhanced significantly with well-aligned AC-EO stagnation lines. Based on the above results, bakers yeast cells were also used to test the trapping concept. As shown in Fig. 10B, cells in pure DI water exhibited a very weak response to the applied voltage (20 V_{RMS}, 400 kHz), and after 15 min, there was a negligible collec-

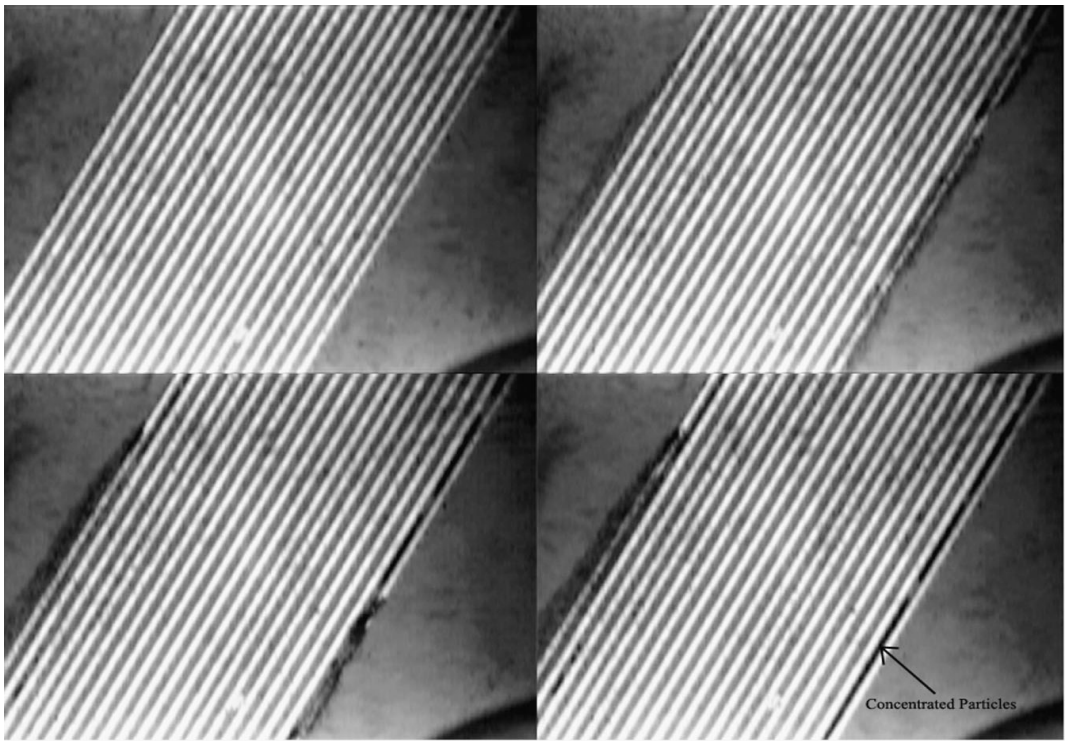

Figure 9. Images of 5 μm particle collection over a period of 35 s for 20 V_{RMS} and 400 kHz: top left image, 0 s; top right, 10 s; bottom left, 20 s; bottom right, 32 s.

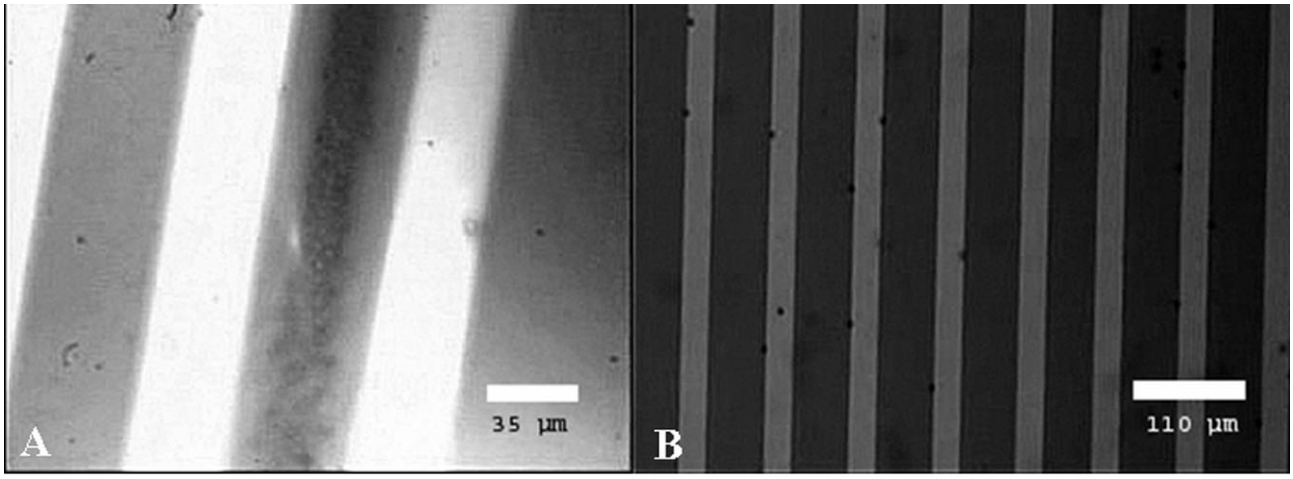

Figure 10. n-DEP behavior of yeast cells with the addition of zwitterions (A) and no zwitterions added (B) at 20 V_{RMS} and 400 kHz.

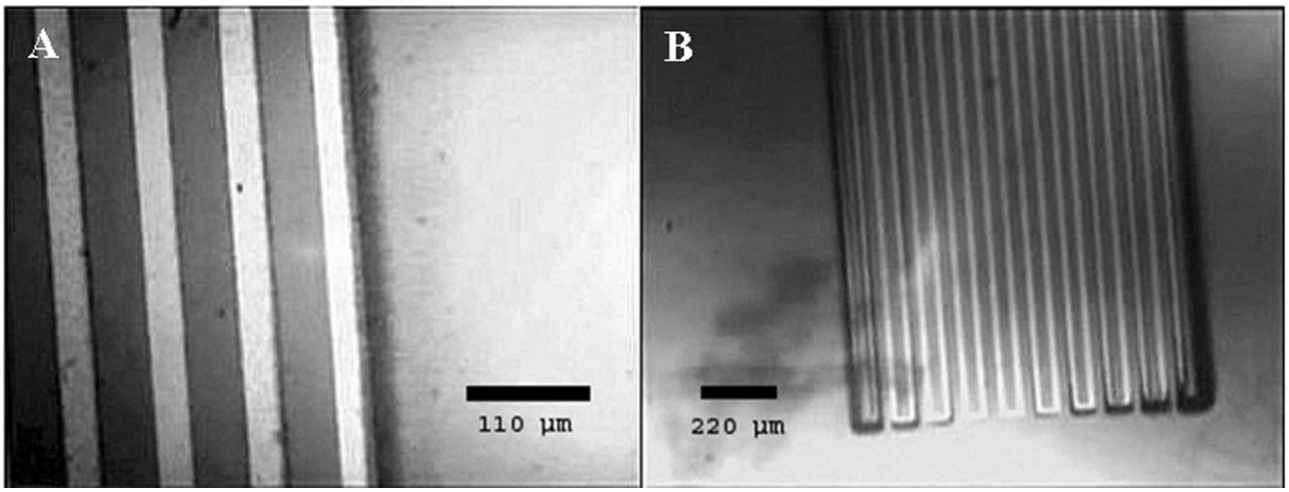

Figure 11. (A) Convection-enhanced bacteria accumulation on high field region of wire after 12 s at 20 V_{RMS} and 400 kHz. (B) Full view of device after 30 s indicates highly concentrated regions of bacteria at the high field edges of the device.

tion. However, as illustrated in Fig. 10A, the addition of a 1.5 M solution of zwitterion to the suspension under identical conditions led to a collection of yeast cells in the stagnation aligned field minimum in approximately 12 s, which is very rapid for the large sample volume of 70 µL.

E. coli bacteria (F-amp) at a concentration of approximately 500 CFU/mL, suspended in an aqueous solution of 1.5 M AHA, were also tested. The device was operated at 20 V_{RMS} and 400 kHz, and as shown in Fig. 11A, after approximately 12 s, the bacteria were concentrated on the high field region at the edge of the rightmost wire. More importantly, they appear to preferentially collect on the outside wire edge, as opposed to the inside edge. Referring to Fig. 4, it is clear that there exists strong tangential EO flow over the wire surface and any bacteria in the bulk solution can be convected across the substrate surface to a wire edge from either the left or the right, where they can then be trapped at a high field region. From the calculated fluid velocity profile, any bacteria approaching from the right will be first exposed to a region of high field at the outer wire edge of the rightmost wire, while any bacteria approaching from left will be convected towards the wire to the left of the rightmost wire and into a region of field minimum. Because the bacteria are repelled from regions of low field, and cannot oppose fluid convection, they will be introduced into the fluid streamlines above the rightmost wire, where they will be convected, and trapped at the high field wire edge.

Figure 11B shows a full view of the device after 30 s and clearly shows the accumulation of bacteria on the high field regions of the wire.

Because the device has well-defined field minimums and maximums in the vicinity of strong AC-EO flow, an experiment was carried out in order to observe the separation abilities of the device. A dilute suspension of 1 and 5 μm microspheres in a 1.5 M AHA solution was injected into the microchannel. Shown in Fig. 12A, when the device was operated at 20 V_{RMS} and 400 kHz, the 1 μm polystyrene particles were attracted to the high field wire corners, while the 5 μm latex particles were attracted to the low field gap between the two wires. It is clear from this picture that the COF is particle size-dependent. The fact that the 5 μm particles have a lower COF than the 1 μm particles at least qualitatively verifies the COF scaling arguments described earlier.

The experiment was repeated under identical voltage frequency conditions with a suspension of 1 and 5 μm microspheres in DI water. Shown in Fig. 12A, the 1 μm particles collect in the same manner, however the 5 μm particles are convected to the stagnation region, where they are locally repelled by the n-DEP trap. This is seen in Fig. 12B as a concentrated region of 5 μm particles are levitating above the trap, most likely due to a balance between convective and DEP forces.

The device was also used for particle manipulation. A dilute solution of 5 μm latex particles in 1.5 M AHA was placed in the microchannel and a voltage was applied (20 V_{RMS}, 500 kHz) for 4 min, which provided ample time for the microparticles to collect on both sides of the device. Following the collection, the applied signal frequency was adjusted in a step-change manner from 500 to 50 kHz and the particles were observed to lift off from the substrate and become reintroduced into the velocity field. As shown in Fig. 13, the particles are seen to lift off and two plugs of particles appear to approach each other. The plug on the left then overshoots the plug on the right, which gets trapped on the serpentine wires.

The step change in frequency from 500 to 50 kHz causes the trapped particles to cross-over from n-DEP to p-DEP. At 50 kHz, the once highly attracting field minimum is a highly repulsive region, which forces the particles outward where they are reintroduced into the velocity field. In looking at the calculated velocity profile, shown in Fig. 3, it is clear that if trapped particles are repelled from the field minimum, they will follow the fluid streamlines until they reach a more favorable location (p-DEP trap). The particles on the right side of the device will be forced upward and to the left, while the particles on the right will be convected across the surface of the device. In looking down on the device, it would appear that the particles move towards each other, however careful imaging, shown in Fig. 13, shows that the particles originally trapped on the right-hand side of the device clearly flow above the particle slug arriving from the left. Additionally, because the particles on the left are convected across the device surface, and are acting under p-DEP, they are immediately trapped on the high field wires, while that of the right-hand slug continues to flow over the device. These images clearly support the calculated velocity profile over the device and that particles can be manipulated to different field regions by exploiting their COFs.

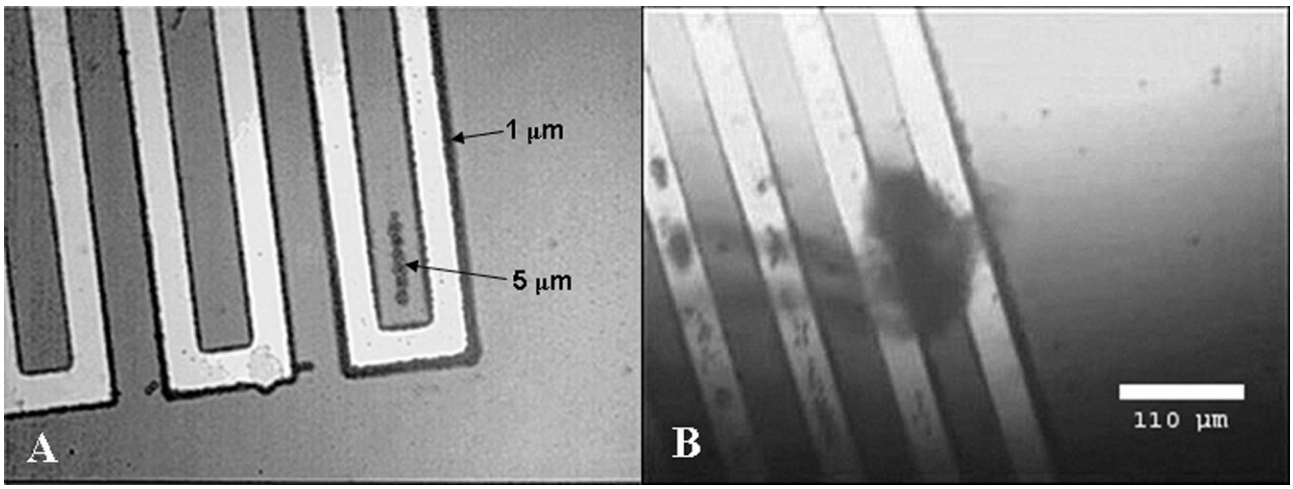

Figure 12. (A) 1.5 M AHA, 1 μm particles experiencing p-DEP at 20 V_{RMS} and 400 kHz and attracted to wire edges, 5 μm particles experience n-DEP, attracted to wire gap. Image taken after 15 s. (B) DI water, 1 μm particles experience p-DEP, 5 μm particles repelled from field minimum at the same voltage and frequency.

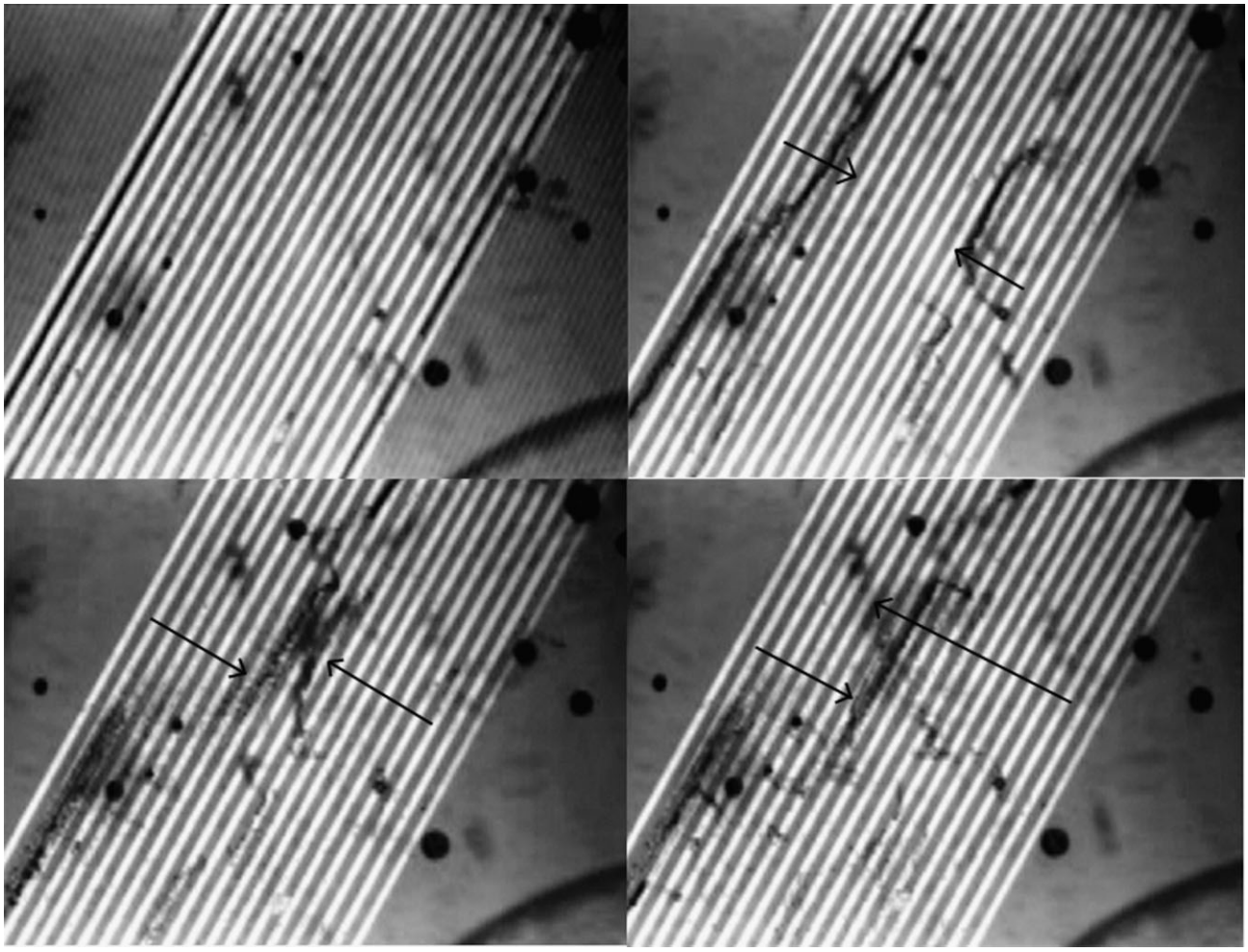

Figure 13. Rapid particle release: Top left, 0 s; top right, 0.25 s; bottom left, 0.50 s; bottom right, 1 s. Careful look at bottom right image shows the right particle slug overshooting the left particle slug. Applied voltage is 20 V_{RMS} and the applied frequency is 500 kHz.

Finally, experiments were performed to study the device in the high voltage regime. A solution of 1.5 M AHA was injected into the microchannel and a potential of 2500 V_{RMS} at a frequency of 500 kHz was dropped across the wire. Within seconds two large counterrotating vortices were observed on each end of the serpentine wire device. This type of fluid motion is expected and is consistent with all the previous work involving AC-EO generated fluid flows. Prior to applying the potential to the wire, the backside of the silicon substrate temperature was measured to be 24.45°C. While no vapor formation was observed in the microchannel during operation, the substrate temperature increased, and in approximately 10 s after the voltage was applied, achieved an equilibrium value of 35.4°C. A high voltage probe was placed across the device and the voltage drop across the serpentine wire was measured to be ~2455 V_{RMS}. The device was continually operated for a period of 2 h and during this time the substrate temperature increased to 37.2°C, however no Faradaic reactions were observed and the device demonstrated stable operation.

A second experiment was performed in order to determine under what conditions Faradaic reactions are produced by the wire. A solution of 1.5 M AHA was subjected to 2500 V_{RMS} at varying frequencies and was observed for any evidence of Faradaic reactions. Initially, when operating at 500 kHz, no reactions were observed. The frequency was slowly decreased from 500 to 132 kHz, where significant bubble generation was observed. Increasing the frequency from 132 to 200 kHz immediately stopped bubble formation.

The fact that no significant heat, bubble, and vapor generation was observed at high frequencies indicates that there is no significant Faradaic reactions being generated

by the wire device. This is surprising given the high applied voltage. However, based on the experiments we believe reactions are negligible because of the combination of high AC frequency and the cross-section geometry of the wire.

4 Concluding remarks

This paper proposes an improved method over conventional DEP techniques and earlier AC-EO traps for collecting, separating, and manipulating various types of micron size particles in suspension. By designing a serpentine device that allows a high voltage to be applied and by tuning the permittivity of a particle suspension using ionic molecules, optimum conditions can be achieved where there exists strong electroosmotic convection (~1 mm/s) over a large volume of electrolyte (70 μL) within a frequency range where particles can exhibit both n-DEP and p-DEP. By aligning fluid stagnation lines directly on local field minima and maxima and by aligning their characteristic frequencies with zwitterions, the required time to trap particles was reduced by two orders of magnitude. Additionally, the rapid concentration of bakers yeast cells and *E. coli* bacteria was also established. The concept of an enhanced separation technique was demonstrated. The critical factor for aligning the frequencies of AC-EO and DEP for convection-enhanced trapping is the electrolyte permittivity and double layer conductivity, and this work has produced several unanswered questions that need future investigation. For example, the permittivity of the electrolyte is assumed to be affected by AHA, however it is unknown as to how this ionic molecule affects the permittivity of the particle surface, or the membrane of a cell or bacterium. The observed decrease in particle COF could have been caused by a modification of both electrolyte and particle permittivity brought on by the zwitterions. These ions could also change the double layer conductivity of the particles and hence produce a tangential conduction effect not related to the permittivity and not included in the classical DEP theory discussed in this work. Such detailed considerations will be analyzed with a parallel theoretical study. Finally, the serpentine device appears to generate high electric fields without observable Faradaic reactions. While this is counterintuitive, experiments indicate that high-frequency AC wire operation appears to be responsible for reaction elimination. However, a more detailed study needs to be performed in order to validate why a continuous wire structure can sustain voltages on the order of kilovolts without boiling or electrolyzing the fluid sample.

Received February 16, 2005
Revised June 21, 2005
Accepted June 23, 2005

5 References

[1] Ivnitski, D., Abdel-Hamid, I., Atanasov, P., Wilkins, E., *Biosens. Bioelectr.* 1999, *14*, 599–624.

[2] Auersward, J., Knapp, H. F., *Microelectron. Eng.* 2003, *67*, 879–886.

[3] Gomez, R., Bashir, R., Sarikaya, A., Ladisch, M. R., Sturgis, J., Robinson, J. P., Geng, T., Bhunia, A. K., Apple, H. L., Wereley, S., *Biomed. Microdevices* 2003, *3*, 201–209.

[4] Morgan, H., Hughes, M. P., Green, N. G., *Biophys. J.* 1999, *77*, 516–525.

[5] Pethig, R., Hughes, M. P., *Anal. Chem.* 1999, *71*, 3441–3445.

[6] Arnold, W. M., Schwan, H. P., Zimmermann, U., *J. Phys. Chem.* 1987, *91*, 5093–5098.

[7] Suehiro, J., Hamada, R., Noutomi, D., Shutou, M., Hara, M., *J. Electrostat.* 2003, *57*, 157–168.

[8] Hoettges, K. F., McDonnell, M. B., Hughes, M. P., *J. Phys. D* 2003, *36*, L101–L104.

[9] Wu, J., Ben, Y., Battigelli, D., Chang, H.-C., *Ind. Eng. Chem. Res.* 2005, *44*, 2815–2822.

[10] Wong, P. K., Wang, T.-H., Deval, J. H., Ho, C.-M., *IEEE/ASME Trans. Mechantronic* 2004, *9*, 366–376.

[11] Green, N. G., Ramos, A., Gonzalez, A., Morgan, H., Castellanos, A., *Phys. Rev. E* 2000, *61*, 4011–4018.

[12] Jones, T. B., *Electromechanics of Particles*, Cambridge University Press, Cambridge 1995.

[13] Pohl, H. A., *Dielectrophoresis*, Cambridge University Press, Cambridge 1978.

[14] O'Konski, C. T., *J. Phys. Chem.* 1960, *64*, 605–619.

[15] Gonzalez, A., Ramos, A., Green, N. G., Castellanos, A., Morgan, H., *Phys. Rev. E* 2000, *61*, 4019–4028.

[16] Ben, Y., Chang, H.-C., to appear in *CRC Handbook of MEMS*, 2005.

[17] Arnold, W. M., Zimmermann, U., *Biochem. Soc. Trans.* 1993, *21*, 475S.

[18] Morgan, H., Green, N., *AC Electrokinetics: Colloids and Nanoparticles*, Research Studies Press, Hertfordshire, England 2003.

[19] Drazin, P. G., Reid, W. H., *Hydrodynamic Stability*, Cambridge University Press, Cambridge 1981.